InSb Avalanche Photodiodes on GaAs Substrates for Mid-Infrared Detection

Y. Alimi[1], V. Pusino[1,2], Matthew J. Steer[1], and D.R.S. Cumming[1,2], *Member, IEEE*

***Abstract*— We present indium antimonide-based devices for mid-infrared detection with enhanced sensitivity. InSb devices will be useful for many applications such as gas sensing and imaging. InSb avalanche photodiodes monolithically integrated with GaAs substrates were fabricated with diameters ranging from 90 to 200 µm, and extensively characterised at temperatures ranging from 77 K to 300 K. At 120 K a zero-bias responsivity of 2 A/W was measured, corresponding to a quantum efficiency of 55%. An experimental gain value of 10 at a reverse bias of -3 V was obtained at 120 K, which to the best of our knowledge is the highest ever reported for InSb avalanche photodiodes. These results pave the way for the development of monolithically integrated mid-infrared array with added gain and wavelength tunability.**

***Index Terms*—Indium compounds, Infrared sensors, Photodetectors, Semiconductor devices**

I. Introduction

The mid-infrared (mid-IR) region is of great interest for sensing applications, since the absorption lines of molecules such as carbon dioxide, methane, and ammonia are found within this spectral region [1]. Indium antimonide (InSb) and mercury-cadmium telluride (MCT) are well-established platforms for photodiodes (PDs) grown on native substrates, but have high costs. Mid-IR PDs based on different device layers and grown on non-native substrates have also been proposed [2, 3] with the aim of driving down device cost. There is considerable interest into adding new functionalities to the PDs. For an avalanche photodiode (APD) the avalanche process gives internal gain by generating multiple carriers for each absorbed photon, thus increasing the device limit of detection. Mid-IR APDs operating at 77 K have been reported on MCT material [4], on indium arsenide [5] and InSb [6]. Here we show avalanche behaviour in an InSb p-i-n structure. Unlike previously reported devices, our InSb p-i-n APD was grown on a semi-insulating (SI) gallium arsenide (GaAs) substrate. Besides the obvious cost-saving aspect of growing on SI GaAs, such heterogeneous growth has allowed the demonstration of monolithic arrays of InSb PDs [7] by functionalising the GaAs layers to make transistors for addressing the detectors. A mid-IR APD on GaAs would thus pave the way towards a monolithically integrated array in the mid-IR with built-in gain and enhanced sensitivity. The article is structured as follows: Section II describes the device layers, the growth and the fabrication process; Section III details the electrical characterisation, carried out both at low temperature (120 K) and at room temperature; Section IV presents the optical characterisation of the InSb APDs; and finally Section V summarises and discusses the experimental results.

II. Device Structure and Fabrication

The InSb APDs measured in this work were fabricated on a heterogeneous epitaxial layer structure where the antimonide layers were grown on top of a SI GaAs substrate by Molecular Beam Epitaxy (MBE). MBE growth on a SI substrate allows separate devices to be completely isolated, which is useful for monolithic integration of electronic circuits, as well as reducing parasitic capacitances for high-frequency and low-power operation. Growth on SI subtrates, however, is more challenging than on doped substrates as the latter suffer less from temperature instability across the wafer [8]. Table 1 details the composition, thickness, and doping of the layers.

TABLE I
DEVICE MATERIAL STRUCTURE

Thickness (nm)	**Material**	**Dopant (type)**	**Carrier Conc. (cm^{-3})**
500	InSb	Be (p+)	5.0E+17
20	$Al_{0.15}In_{0.85}Sb$	Be p+	7.0E+17
2000	**InSb**	Be p+	graded from 5.0E+16 to 7.0E+17 (bottom to top)
3000	**InSb**	Nid n-	5E+15
3000	**InSb**	Te n+	5.0E+17
300	GaSb	Ud	
600	GaAs	Si n+	2.0E+18
300	GaAs	Si n-	1.0E+17
500	GaAs	Ud	
600000	GaAs	Ud	

[1]James Watt School of Engineering, University of Glasgow, U.K.
[2]Corresponding authors: Vincenzo.Pusino@glasgow.ac.uk, David.Cumming.2@glasgow.ac.uk
Dataset Digital Object Identifier: 10.5525/gla.researchdata.888

The layer structure is very similar to that reported in [2]. However, there are two key changes: the absorption region is heavily doped to ensure most of the incident radiation is absorbed and converted into electron-hole pairs; an undoped avalanche region was introduced between the absorption region and the underlying InSb n-contact layer to sustain the avalanche of the photo-generated carriers. The changes to the epitaxial layer structure reflect the fundamental differences in operation between a PD and an APD. In a PD, the heavily doped upper contact layer, necessary to make good Ohmic contacts, is made as thin as possible to reduce unwanted photon absorption and ensure photons are instead absorbed in the underlying absorption layer that is left undoped. On the other hand, in an APD, the absorption layer is intentionally thicker and heavily doped in order to absorb nearly 100 % of the incident radiation. The high electric field in the avalanche region then causes impact ionisation to take place, resulting in a multiplication of the photo-generated carriers. The avalanche region needs to be carefully designed both in terms of thickness and doping, as the electric field across this layer must remain constant, to maximise the avalanche gain and avoid device breakdown due to high field gradients at the interfaces between layers. Simulations showed how changes to several material parameters affect the electric field across the avalanche region [9], highlighting that a very accurate control of thickness and doping of the avalanche region is needed to attain good APD performance. A similar material structure has been reported for InSb APDs grown on an n-doped InSb substrate [6]. The previously reported structure did not have the $Al_{0.15}In_{0.85}Sb$ barrier that provides a better rectifying behaviour, especially as the temperature is increased towards room temperature. The conduction band barrier height provided by the $Al_{0.15}In_{0.85}Sb$ layer is estimated to be greater than 80 meV [10].

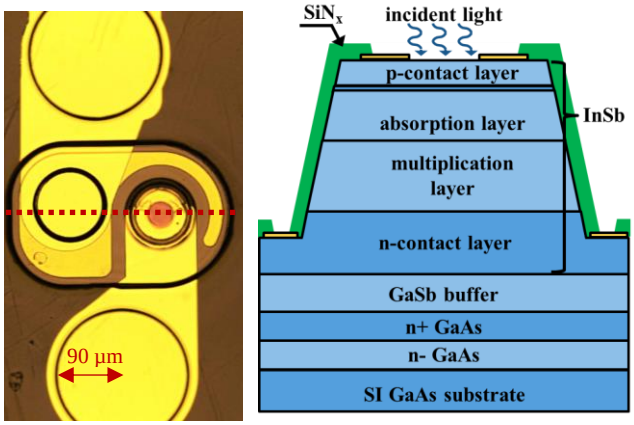

Fig. 1. (a) Optical micrograph of a 90 µm diameter InSb APD. The dashed red line indicates the section along which the cross-sectional diagram (b) of a completed device is presented.

Circular photodiodes with mesa diameters ranging from 90 µm to 200 µm were fabricated on the InSb APD material using a similar fabrication process to that used for InSb PDs, the details of which have been given elsewhere [2]. Fig. 1(a) shows an optical micrograph of one of the finished devices before wire-bonding, whereas the diagram in Fig. 1(b) illustrates the cross section of a finished APD. Devices were isolated by etching the material surrounding the InSb n-contact down to the SI GaAs substrates. A 600 nm-thick layer of silicon nitride (SiN_x) was used to passivate the devices and minimise sidewall-related leakage current.

III. Electrical Characterisation

Dark *I-V* characterisation of the InSb APDs was carried out at three different temperatures (77, 120 and 300 K) using a Keysight B1500 Source Meter Unit (SMU). Devices with various mesa diameters were measured, ranging from 90 to 180 µm. The heavily doped GaAs layers present in the structure do not affect the *I-V* characterisation of the InSb APDs, due to the thick GaSb buffer interposed between the two materials. Fig. 2 (a) and (b) show the dark current and the dark current density as a function of the applied bias voltage for an APD with a diameter of 90 μm.

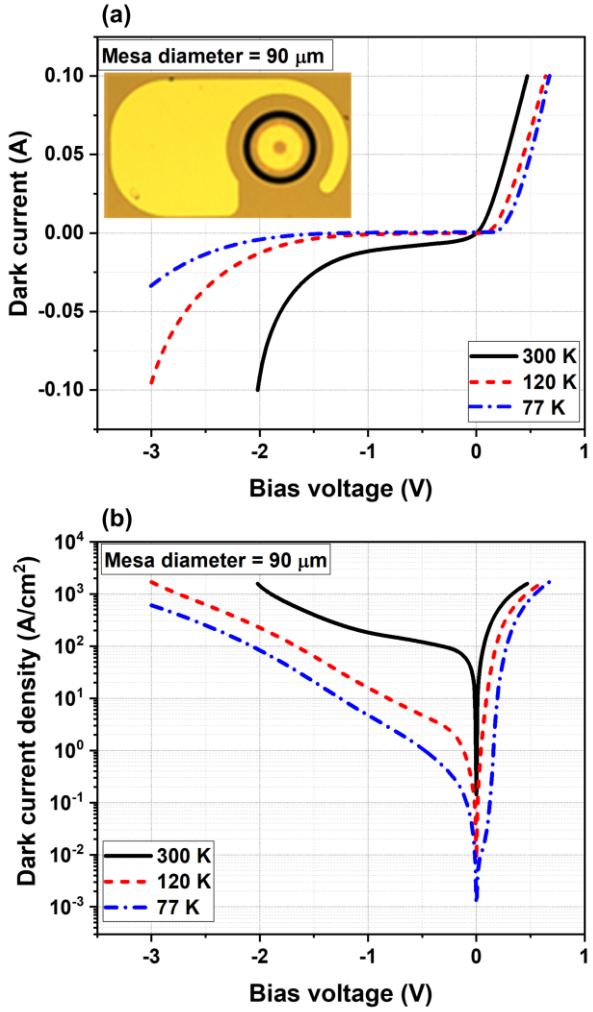

Fig. 2. *I-V* characterisation results showing (a) the dark current and (b) the dark current density of a 90 µm diameter InSb APD measured at 77 K, 120 K and 300 K.

The rectification behaviour of the APD improves as the temperature decreases, with the smallest values of leakage current observed at 77 K. The dark current density measured at -50 mV is 36.8 A/cm^2 at 300 K, and reduces to 0.23 and

0.038 A/cm^2 at 120 and 77 K, respectively. The values are consistent with the residual doping level of 5E+15 cm^{-3} of the intrinsic avalanche region [9]. The *I-V* characterisation results suggest that thermal processes such as Shockley-Read Hall (SRH) and Auger generation of intrinsic carriers in the depletion region become the main mechanisms of leakage current generation as the temperature increases towards 300 K. The 20 nm-thick p+ $Al_{0.15}In_{0.85}Sb$ barrier layer suppresses the diffusion of thermally generated carriers from the upper contact region into the intrinsic region [11,12], but thermal excitation in the intrinsic region will still be present. As one would expect, the contribution of thermally generated carriers to the leakage current decreased with the temperature and the bandgap of InSb correspondingly increased from 180 meV at 300 K to 227 meV at 77 K [13,14]. The effect of surface leakage (shunt current) and band-to-band tunneling was more significant at higher reverse bias, and was negligible at zero or low bias voltages [15].

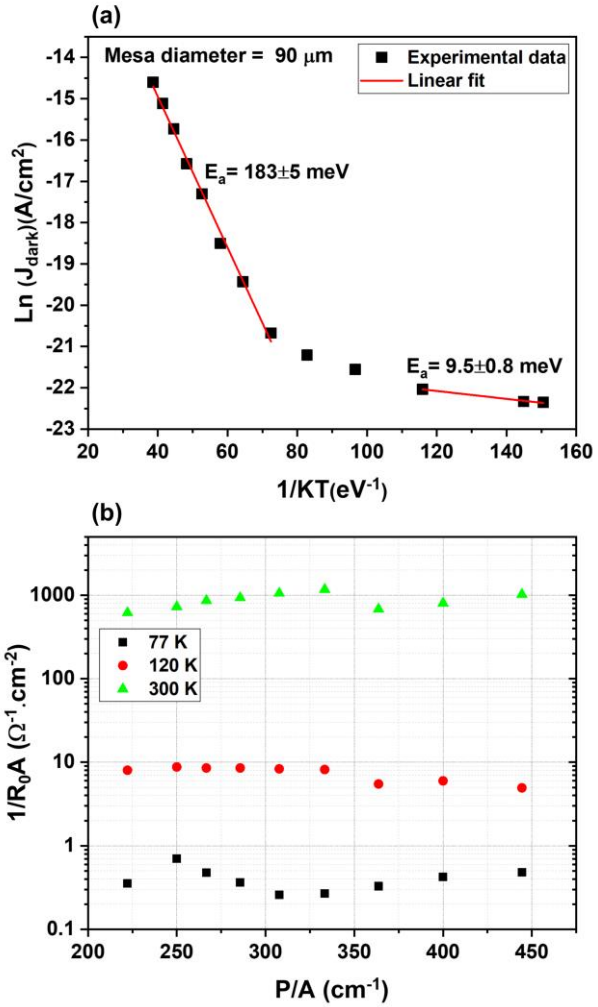

Fig. 3. (a) Arrhenius plot of a 90 µm diameter InSb APD and (b) 1/ R_0A plotted as a function of perimeter/area.

The Arrhenius plot in Fig. 3 (a), showing the dark current density at a bias of -50 mV vs. the temperature for the 90 µm mesa APD, provides further insight into the dominant dark current generation mechanism at different temperatures. As Fig. 3 (a) shows, the activation energy of electrons (E_a) was extracted from the slope of the curve, with two values obtained for different temperature intervals. From room temperature down to approximately 160 K, E_a is estimated to be 183 meV, which is close to the bandgap of InSb [13,14]. The two Auger generation processes most relevant to InSb (Auger 1 and Auger 7) have threshold energies close to the bandgap of InSb [16], thus the measured value of E_a suggests that their contribution to the leakage current dominates over SRH in this temperature range. Below 100 K, E_a is 9 meV, which is significantly lower than the band gap of InSb. The low value of E_a suggests surface leakage currents and/or shallow energy traps dominate dark current generation between 77 and 100 K [17]. Since the sidewalls of the APDs were passivated with SiN_x, it is thought the main contribution arises from shallow traps related to threading dislocations and growth defects.

The zero-bias resistance (R_0) is the differential resistance at zero bias extracted from the dark *I-V* characteristic. The zero-bias resistance-area product (R_0A) is often used as a figure of merit for photodetectors and it can be used to understand the bulk and surface leakage contribution to the dark current. Fig. 3 (b) shows $1/R_0A$ as a function of perimeter-to-area ratio (P/A). The relationship between $1/R_0A$ and P/A follows the equation [14]:

$$\frac{1}{R_0A} = \frac{1}{R_0A_{bulk}} + \frac{1}{r_{surf}}\frac{P}{A} \quad (1)$$

where R_0A_{bulk} is the bulk contribution to the R_0A, and r_{surf} is the surface resistivity. As it can be clearly seen from Fig. 3 (b), $1/R_0A$ is nearly constant across the range of devices measured, suggesting the surface resistivity component in eq. (1) can be neglected, i.e. the leakage current attributed to surface states has been effectively suppressed through SiN_x passivation.

IV. Optical Characterisation

The absorption spectra of the APDs in the mid-IR range were measured using a Fourier Transform infrared (FTIR) spectrometer (Bruker Vertex 70) at 300 K and 120 K. The zero-bias absorption spectra of an APD with a mesa area of 90 µm measured at 120 and 300 K are shown in Fig. 4, and devices with different areas showed similar results.

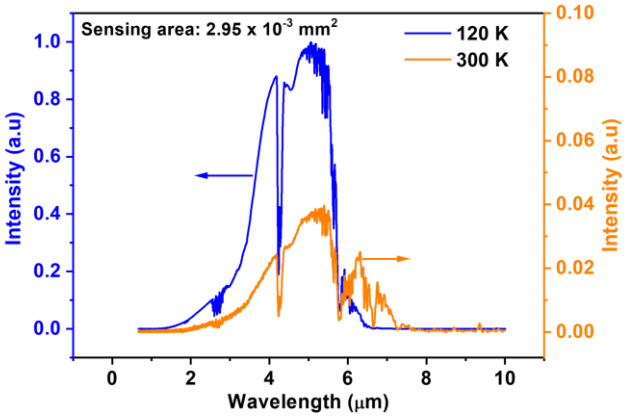

Fig. 4. Comparison of absorption spectra of a 90 μm diameter InSb APD at 120 and 300 K.

The spectra of all devices measured presented cut-off wavelengths of 6.3 and 7.7 μm at 120 and 300 K, respectively, corresponding to the energy bandgap of InSb at those temperatures [13,14]. Moreover, the intensity of the spectrum at 120 K was approximately 80 times higher than that at 300 K, due to the reduced Auger recombination and increased carrier lifetime at lower temperature [13]. The dip in the spectrum at 4.2 μm is because of the spectral absorption of carbon dioxide molecules, as the experiments were carried out in the ambient room environment.

The responsivity performance of the APDs was also studied at 120 and 300 K, using a continuous-wave distributed feedback (DFB) Quantum Cascade Laser (QCL) from Hamamatsu (L12004-2190H-C) as a mid-IR source with peak wavelength of 4.57 μm. The responsivity (R_I) of the APDs is calculated as:

$$R_I = I_{ph}/P_{in} = (I_{ph}/P_{total})(A_{beam}/A_{APD}) \quad (2)$$

where I_{ph} is the photocurrent, P_{in} is the laser power incident onto the APD, P_{total} and A_{beam} are respectively the total power and the total area of the laser beam shone on the device, and A_{APD} is the sensing area of the APD (i.e. the total mesa area minus the contact area). The total power of the laser (P_{tot}) was measured with a broad area power meter (Thorlabs S401C, connected to the PM100D control unit), while the size of the beam was obtained using the knife-edge method [18]. The size of the QCL beam was considerably larger (four orders of magnitude) than the sensing area of the devices. Therefore, to ensure the measured responsivity was solely the response of individual APDs, a 150 μm pinhole was placed between QCL and APDs to suppress the effect of internal reflections of the mid-IR radiation in the surrounding semiconductor. Fig. 5 displays the responsivity as a function of sensing area, together with the corresponding quantum efficiency (QE).

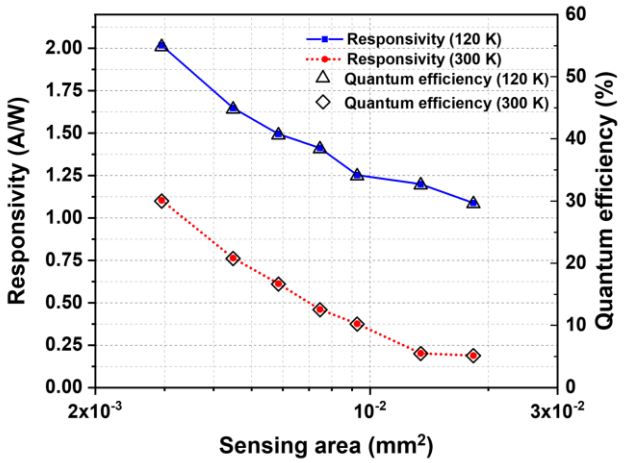

Fig. 5. Responsivity (left axis) and quantum efficiency (right axis) of the InSb APDs at zero bias as a function of device sensing area.

It can be clearly seen that APDs demonstrate higher responsivity (and QE) at 120 K which is a result of increased carrier lifetime and thus larger photocurrent when illuminated. The dominant mechanism limiting room-temperature carrier lifetime in intrinsic InSb is Auger recombination, which is decreased at reduced temperature [12]. Zero-bias QE of a 120 μm APD measured at 120 K and 300 K is 55% and 30% respectively, the latter showing a good agreement with the reported results on InSb photodiode on GaAs [2]. The decrease in responsivity when the sensing area is increased is attributed to the current spreading length remaining constant as the device size is increased, since the InSb APDs have a single annular anode on the top surface of the device (see Fig. 1). Non-uniform current spreading, caused by the much higher p-type sheet resistance compared to the n-type sheet resistance, means that the photo-generated current is collected only in close proximity to the edge of the contact [19]. This current localisation effect is less obvious at low temperature as the current spreading length increases with cooling the APDs [20].

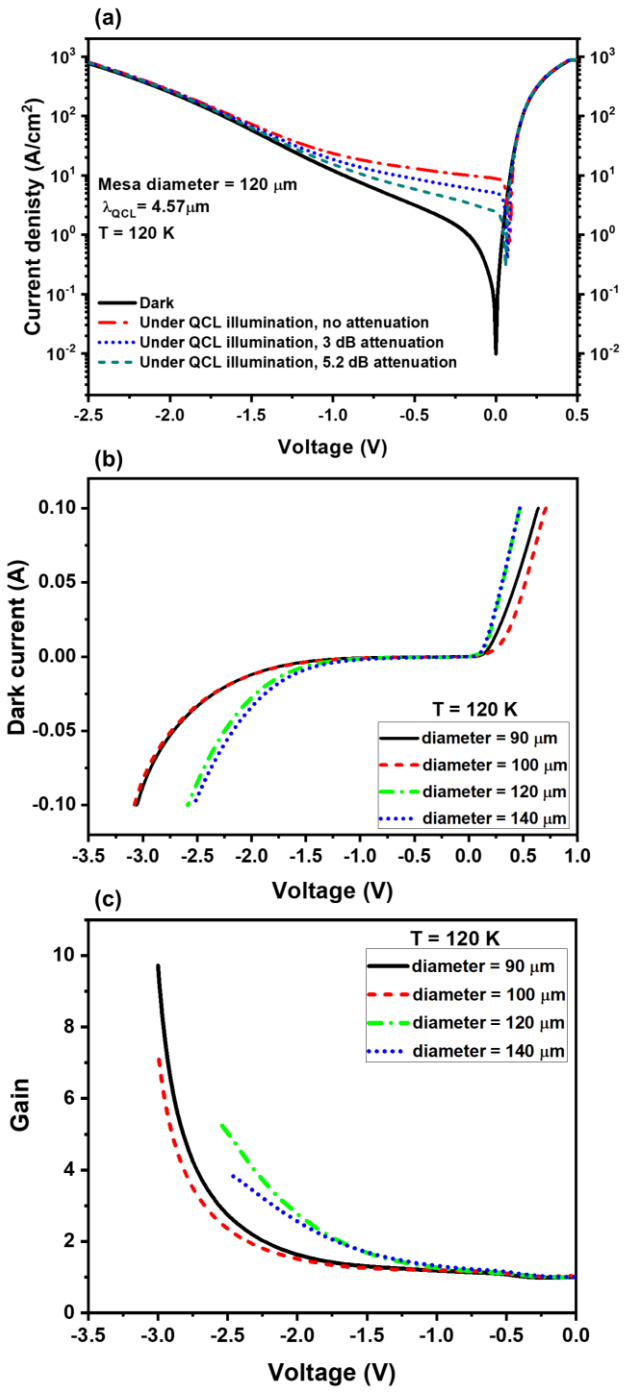

Fig. 6. (a) Current density vs. applied voltage for the 120 μm mesa InSb APD in the dark and under illumination with different photon fluxes; (b) *I-V* characteristics without illumination and (c) gain obtained vs. applied voltage for the four smallest APDs fabricated.

The gain of the InSb APDs was also measured. The gain of an APD with a reverse bias V applied is defined as the ratio of the generated photocurrent at the bias voltage $I_{ph}(V)$ to the zero-bias photocurrent $I_{ph}(0)$ as given by [9,11]:

$$G(V) = \frac{I_{ph}(V)}{I_{ph}(0)} = \frac{I_{illuminated}(V) - I_{dark}(V)}{I_{illuminated}(0) - I_{dark}(0)} \quad (3)$$

where $I_{illuminated}$ (V) and I_{dark} (V) are the total current under illumination and the dark current at bias voltage V. $I_{illuminated}$ (0) and I_{dark} (0) are the total current under illumination and the dark current at zero bias, respectively.

To measure the gain, the APDs were illuminated by the QCL source and the devices were biased by Keithley 4200 SMU. The photocurrent of all devices was measured under QCL illumination, and neutral density filters (NDFs) were used to attenuate the laser beam and verify that the gain was independent of photon flux. Fig. 6 (a) displays the current density of a 120 μm diameter APD measured at 120 K as a function of the applied reverse bias. It can be seen that the curves under illumination show a good overlap especially towards higher reverse voltages. Fig. 6 (b) and (c) show the dark *I-V* characteristic of the four smallest APDs fabricated, and the corresponding gain that was measured, respectively. A gain of up to nearly 10 at -3 V (i.e. with an electric field of 10 kV/cm across the avalanche region) was obtained for the smallest APD measured. Lower gain was measured for devices with bigger areas, but all fabricated devices showed gain. The increasing gain observed in Fig. 6 (c), that is found to be exponentially dependent on reverse bias, is characteristic of avalanche dominated by impact ionisation from electrons, consistent with previous reports on InSb avalanche mechanism [6,21]. The majority of the photons are absorbed in the thick and heavily p-doped InSb absorption layer, resulting in a pure injection of electrons into the non-intentionally doped InSb avalanche layer.

V. Discussion and Conclusions

A novel material structure is proposed for the realisation of APDs working in the mid-IR wavelength range. The epitaxial layers were grown on SI GaAs substrates, therefore the material is suitable for monolithically integrated mid-IR arrays [22,23]. The devices are passivated using SiN_x to minimize the contribution of surface leakage to dark current. Extensive electrical characterisation from 77 K to 300 K highlighted that the main contribution to the leakage current above 100 K is thermally excited carriers. The resistance-area (R_0A) product was found to be independent of the perimeter to area ratio (P/A), a finding that confirms the effectiveness of the SiN_x passivation. Zero-bias QE of 55% and 30% was achieved at 300 and 120 K respectively, with a 120 μm APD. Experimental characterisation with a reverse bias applied and 4.57 μm illumination yielded a gain of nearly 10 at -3 V. The results suggest avalanche in InSb APDs is dominated by electrons, with the impact ionisation coefficient of electrons α much greater than the impact ionisation coefficient of holes β (α >> β).

The experimental investigation carried out in this work validates the proposed material structure for InSb APDs, demonstrated for the first time on SI GaAs substrates. Future work will explore the possibilities of monolithic integration with functionalised GaAs layers.

Acknowledgement

This work was supported by the Engineering and Physical Sciences Research Council under Grant EP/M01326X/1 (QuantIC) and Grant EP/R019665/1 (IUK). All the

fabrication described in this paper was carried out at the James Watt Nanofabrication Centre (JWNC) at the University of Glasgow. The authors would like to thank all the staff at the JWNC for their assistance.

REFERENCES

[1] A. Krier, Infrared Methods for Gas Detection, *Mid-Infrared Semiconductor Optoelectronics*. London, U.K., Springer, 2006, pp. 595-610.

[2] V. Pusino, C. Xie, A. Khalid, M.J. Steer, M. Sorel, I.G. Thayne, and D.R.S. Cumming, "InSb Photodiodes for Monolithic Active Focal Plane Arrays on GaAs Substrates," *IEEE Transactions on Electron Devices*, vol. 63, no. 8, pp. 3135-3142, 2016, DOI: 10.1109/TED.2016.2578982.

[3] I. Kimukin, N. Biyikli, and E. Ozbay, "InSb high-speed photodetectors grown on GaAs substrate", *Journal of Applied Physics*, vol. 94, no. 8, pp. 5414-5416, 2003, DOI: 10.1063/1.1611286.

[4] J. Beck, C. Wan, M. Kinch, J. Robinson, P. Mitra, R. Scritchfield, F. Ma, and J. Campbell, "The HgCdTe electron avalanche photodiode," *Journal of Electronic Materials*, vol. 35, no. 6, pp. 1166-1173, June 2006, DOI: 10.1007/s11664-006-0237-3.

[5] A.R.J. Marshall, J.P.R. David, and C.H. Tan, "Impact ionization in InAs electronavalanche photodiodes," *IEEE Transactions on Electron Devices*, vol. 57, no. 10, pp. 2631-2638, 2010, DOI: 10.1109/TED.2010.2058330.

[6] J. Abautret, J.P. Perez, A. Evirgen, J. Rothman, A. Cordat, and P. Christiol, "Characterization of midwave infrared InSb avalanche photodiode," *Journal of Applied Physics*, vol. 117, 244502, 2015, DOI: 10.1063/1.4922977.

[7] C. Xie, M. Aziz, V. Pusino, A. Khalid, M.J. Steer, I.G. Thayne, M. Sorel, and D.R.S. Cumming, "Single-chip, mid-infrared array for room temperature video rate imaging," *Optica*, vol. 4, pp. 1498-1502, 2017, DOI: 10.1364/OPTICA.4.001498.

[8] S. D. Wu, L.W. Guo, Z.H. Li, X.Z. Shang, W.X. Wang, Q. Huang, and J.M. Zhou, "Effect of the low-temperature buffer thickness on quality of InSb grown on GaAs substrate by molecular beam epitaxy," *Journal of Crystal Growth*, vol. 277, nos. 1–4, pp. 21–25, Apr. 2005, DOI: 10.1016/j.jcrysgro.2004.12.141.

[9] J. Abautret, J.P. Perez, A. Evirgen, F. Martinez, P. Christiol, J. Fleury, H. Sik, R. Cluzel, A. Ferron, and J. Rothman, "Electrical modeling of InSb PiN photodiode for avalanche operation," *Journal of Applied Physics*, vol. 113, 183716, 2013, DOI: 10.1063/1.4804956.

[10] T. Ashley, and C.T. Elliott, "Operation and properties of narrow-gap semiconductor devices near room temperature using non-equilibrium techniques," *Semiconductor Science and Technology*, vol. 6, no. 1S, p. C99-C105, 1991, DOI: 10.1088/0268-1242/6/12C/020.

[11] K. Ueno, E.G. Camargo, T. Katsumata, H. Goto, N. Kuze, Y. Kangawa, and K. Kakimoto, "InSb Mid-Infrared Photon Detector for Room-Temperature Operation," *Japanese Journal of Applied Physics*, vol. 52, no. 9, p. 6, Sep. 2013, Art. no. Unsp 092202, DOI: 10.7567/JJAP.52.092202.

[12] T. Ashley, A.B. Dean, C.T. Elliott, A.D. Johnson, G.J. Pryce, A.M. White, and C.R. Whitehouse, "A heterojunction minority carrier barrier for InSb devices," *Semiconductor Science and Technology*, vol. 8, no. 1S, p. S386, 1993, DOI: 10.1088/0268-1242/8/1S/086.

[13] A. Rogalski and M. Razeghi, "Narrow-gap semiconductor photodiodes," in *Proc. SPIE 3287, Optoelectronics and High-Power Lasers and Applications*, San Jose, CA, United States, 1998, pp. 12-14, DOI: 10.1117/12.304467.

[14] J. Camassel and D. Auvergne, "Temperature dependence of the fundamental edge of germanium and zinc-blende-type semiconductors," *Physical Review B*, vol. 12, no. 8, pp. 3258-3267, 1975, DOI: 10.1103/PhysRevB.12.3258.

[15] A. Tevke, C. Besikci, C. Van Hoof, and G. Borghs, "InSb infrared p-i-n photodetectors grown on GaAs coated Si substrates by molecular beam epitaxy," *Solid-State Electronics*, vol. 42, no. 6, pp. 1039-1044, June 1998, DOI: 10.1016/S0038-1101(98)00124-5.

[16] A.R. Beattie, “Quantum Efficiency in InSb”, Journal of Physics and Chemistry of Solids, 1962, vol. 23, no. 8, pp. 1049-1056, 1962, DOI: 10.1016/0022-3697(62)90122-1.

[17] B. W. Jia, K. H. Tan, W. K. Loke, S. Wicaksono, and S. F. Yoon, "Integration of an InSb photodetector on Si via heteroepitaxy for the mid-infrared wavelength region," *Optics Express*, vol. 26, no. 6, pp. 7227-7234, 2018, DOI: 10.1364/OE.26.007227.

[18] J.A. Arnaud, W.M. Hubbard, G.D. Mandeville, B. de la Clavière, E.A. Franke, and J.M. Franke, "Technique for Fast Measurement of Gaussian Laser Beam Parameters," *Applied Optics*, vol. 10, no. 12, pp. 2775-2776, 1971, DOI: 10.1364/AO.10.002775.

[19] L. Meriggi, M.J. Steer, Y. Ding, I.G. Thayne, C. MacGregor, C.N. Ironside, and M. Sorel, "Enhanced emission from mid-infrared AlInSb light-emitting diodes with p-type contact grid geometry," *Journal of Applied Physics*, vol. 117, no. 6, pp. 063101, Feb. 2015, DOI: 10.1063/1.4905081.

[20] Y. F. Lao, P.V.V. Jayaweera, S.G. Matsik, A.G. Unil Perera, H.C. Liu, M. Buchanan, and Z.R. Wasilewski, "Analysis of dark current mechanisms for split-off band infrared detectors at high temperatures," *IEEE Transactions on Electron Devices*, vol. 57, no. 6, pp. 1230-1236, June 2010, DOI: 10.1109/TED.2010.2046065.

[21] R.D. Baertsch, "Noise and Multiplication measurements in InSb avalanche photodiodes," *Journal of Applied Physics*, vol. 38, pp. 4267, 1967, DOI: 10.1063/1.1709114.

[22] M. B. Reine, J.W. Marciniec, K.K. Wong, T. Parodos, J.D. Mullarkey, P.A. Lamarre, S.P. Tobin, K.A. Gustavsen, and G.M. Williams, "HgCdTe MWIR Back-Illuminated Electron-Initiated Avalanche Photodiode Arrays," *Journal of Electronic Materials*, vol. 36, no. 8, pp. 1059-1067, 2007, DOI: 10.1007/s11664-007-0172-y.

[23] A. Singh, V. Srivastav, and R. Pal, "HgCdTe avalanche photodiodes: A review," *Optics & Laser*

Technology, vol. 43, no. 7, pp. 1358-1370, 2011, DOI: 10.1016/j.optlastec.2011.03.009.